Outline

Last week (lecture 7/14):

- Amplificiation and Detection of Microwave fields
- Measurement Induced Dephasing

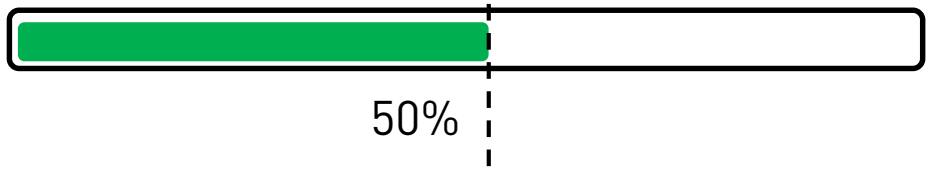

This week (lecture 8):

- Organization lab tour/ Q&A session.
- Summary of last weeks key points.
- 4.10 Control and Characterization of Superconducting Qubits
- 4.11 Sources and mitigation of noise

Summary last week

Microwave field detection

- Realized using linear amplification, down-conversion at a mixer, and direct sampling of the electric field using analog-to-digital conversion.
- Detection scheme equivalent to optical heterodyne detection.
- Measurement observable = complex amplitude $I + iQ$ corresponds to the sum of the signal field b and an additional field h^+carrying the noise.
- Minimal amount of added noise given by vacuum fluctuations.
  - Repeated sampling without any signal results in Gaussian distribution.
- Detection efficiency η limited by performance of first stage amplifier.
- → Use Josephson parametric amplifier to reach up to $\eta \sim 50\%$.

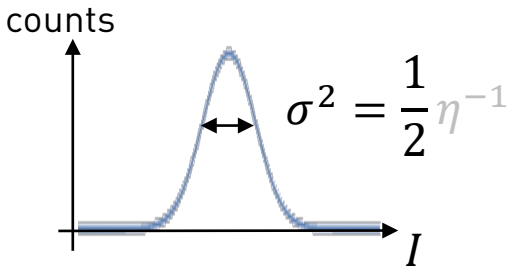

Measurement induced dephasing

- Topic of today's problem set and exercise class.
- Challenge topic: Don't hesitate to ask.

4.10 Control and Characterization of superconducting qubits

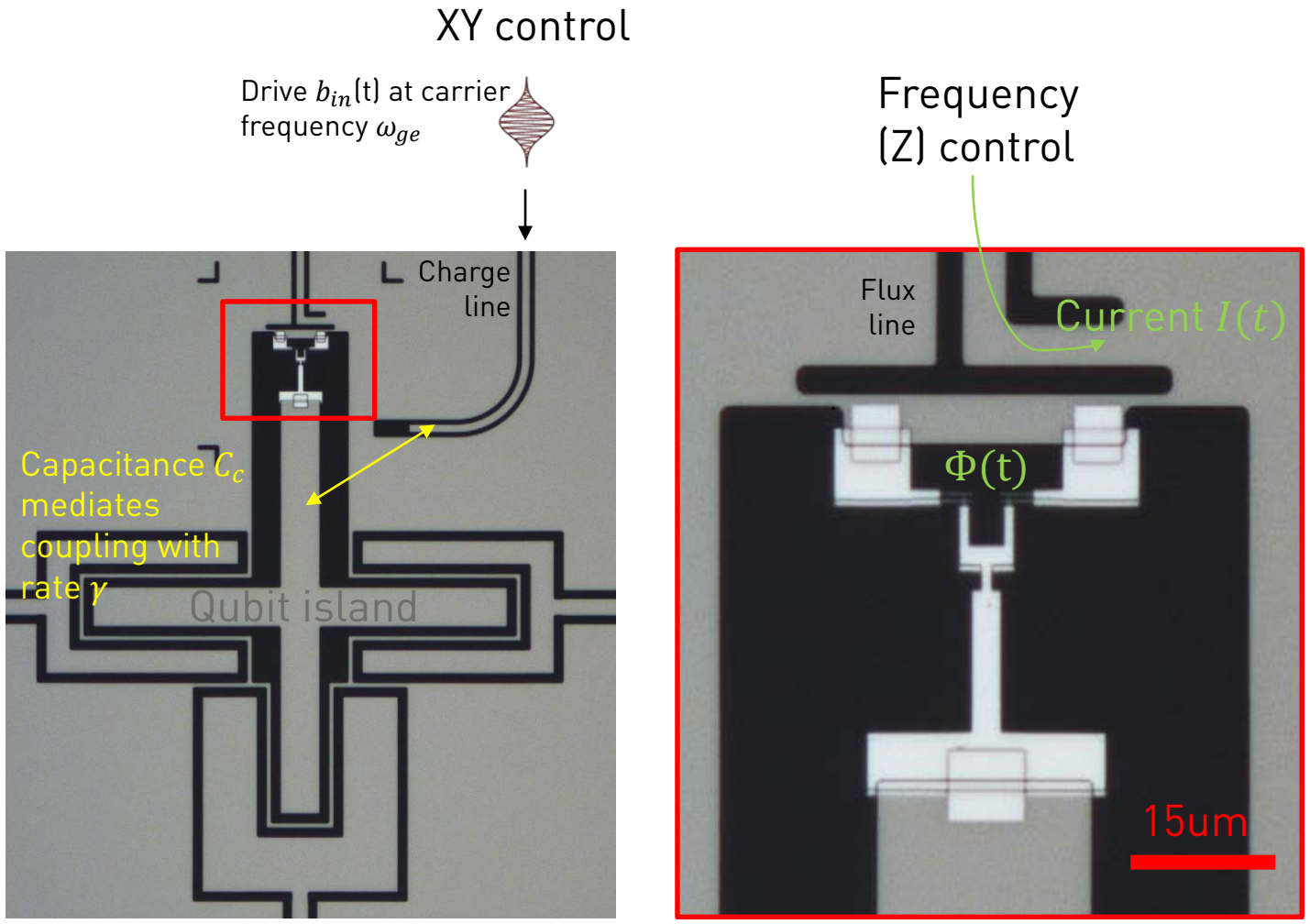

On-chip control

- Microwave drive $b_{in}(t)$ resonant with qubit frequency rotates Bloch vector about X and Y axis. Drive power $P_{in} = \hbar\omega b_{in}^{+} b_{in}$.
- Arbitrary waveform generators (AWG) used to generate pulses, up-converted to the MW frequency band by mixing with a local oscillator field.
- Coupling rate to charge line $\gamma = \frac{C_c^2 Z_0 \omega^2}{C_\Sigma}$ imposes decay and therefore needs to be $\gamma \ll 1/T_1$.
- Tunability of the qubit achieved by sending a current $I(t)$ to a separate control line generating a magnetic flux $\Phi(t)$in the SQUID loop.
- Used for both static (DC) control of the qubit frequency and for applying pulses on nanosecond timescales.

4.10 Control and Characterization of superconducting qubits

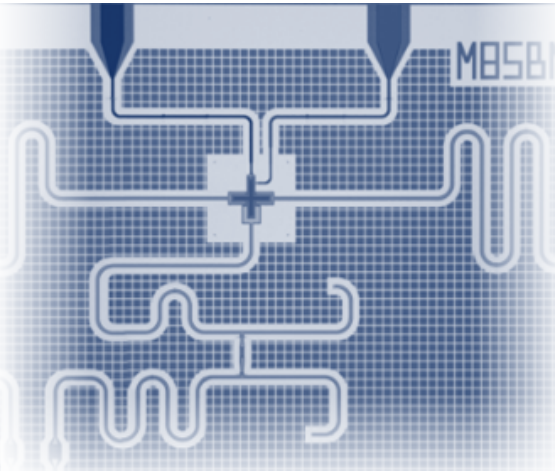

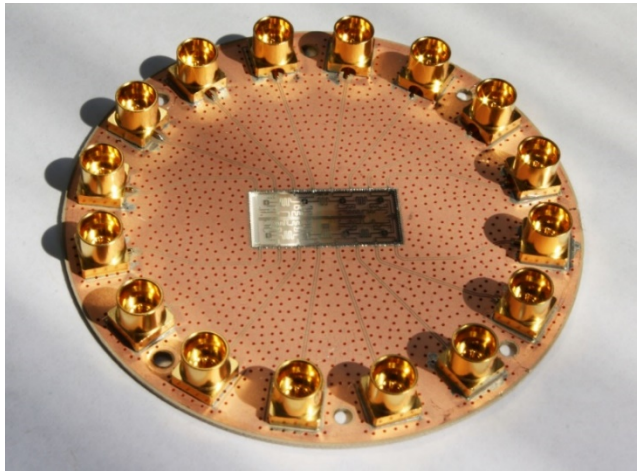

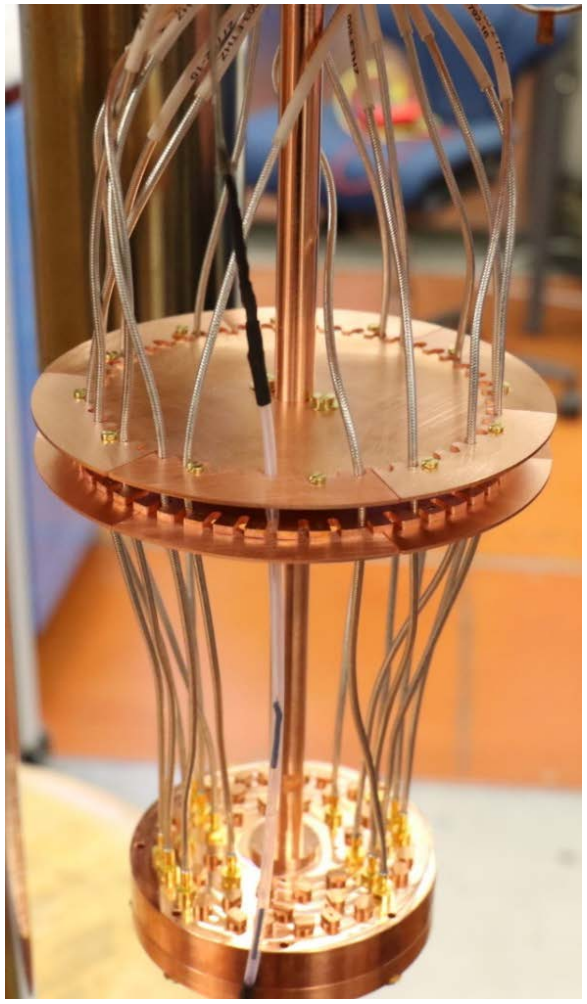

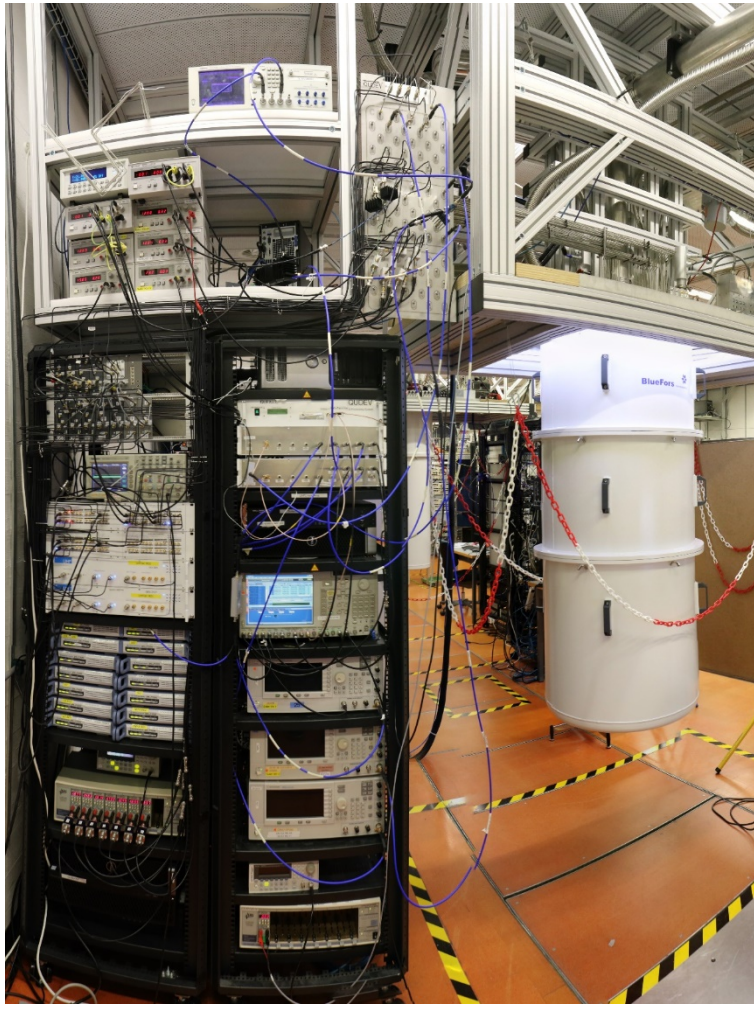

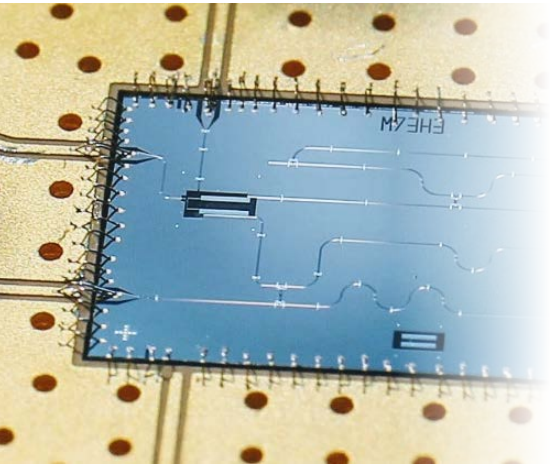

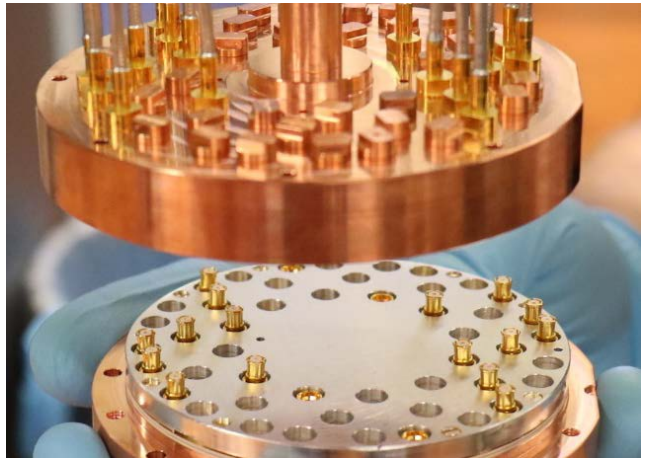

4.10 Measurement of Rabi oscillations

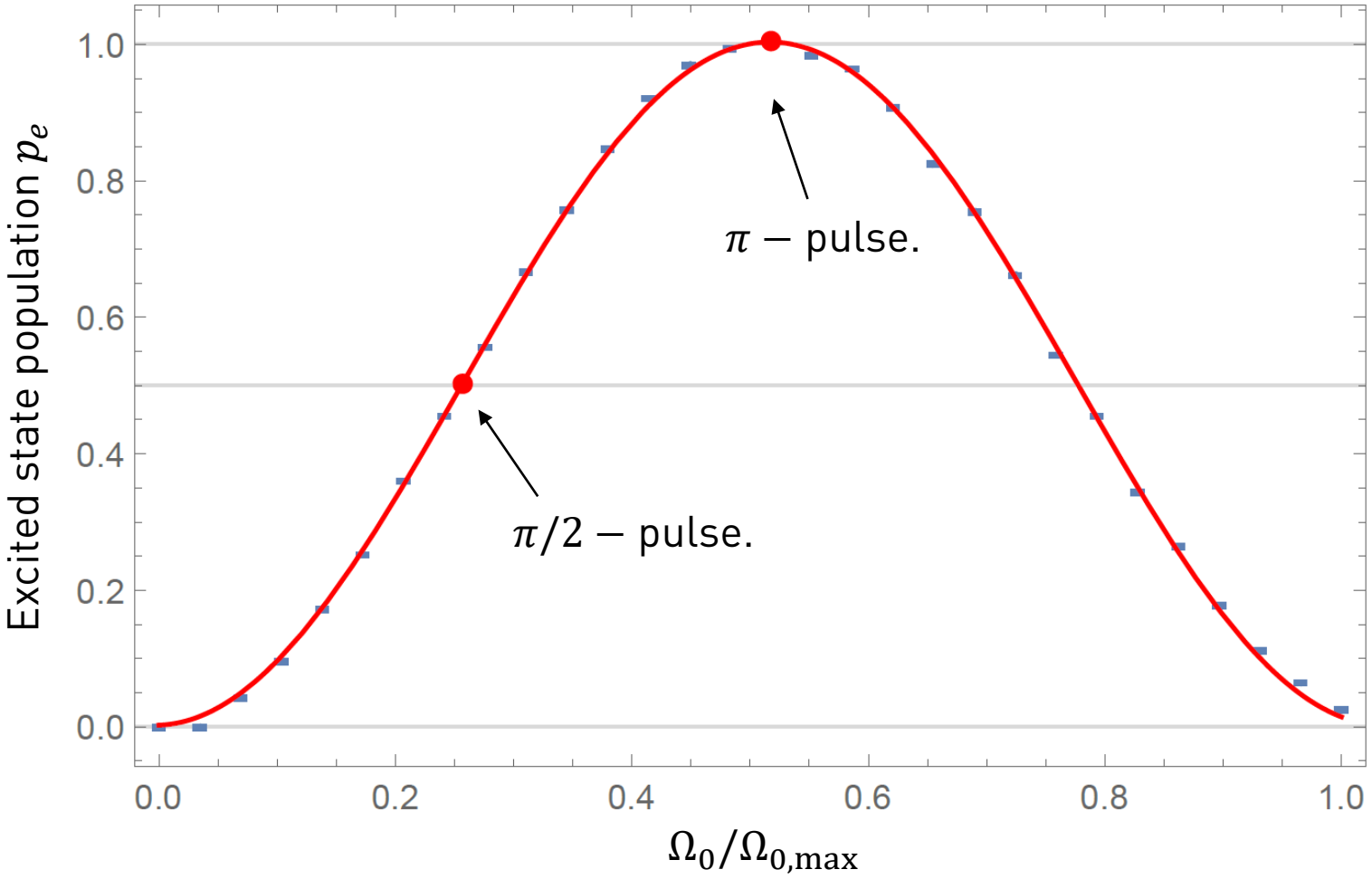

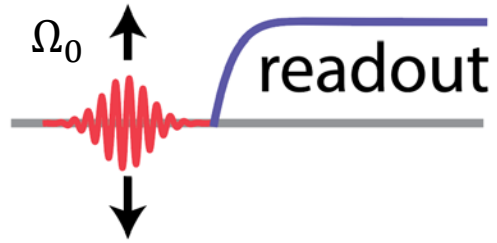

- Qubit frequency $\omega_{ge}/2\pi = 5.758$ GHz determined spectroscopically.
- Initialize qubit in ground state.
- Apply pulse at ω_{ge} with variable amplitude Ω_0.
- Gaussian pulse envelop with characteristic $\sigma \sim 5 - 10ns$.
- Readout qubit state and average over ~10^3 repetitions.
- Sinusoidal fit to extract π- and $\pi/2$-pulse amplitude.

4.10 Measurement of relaxation time

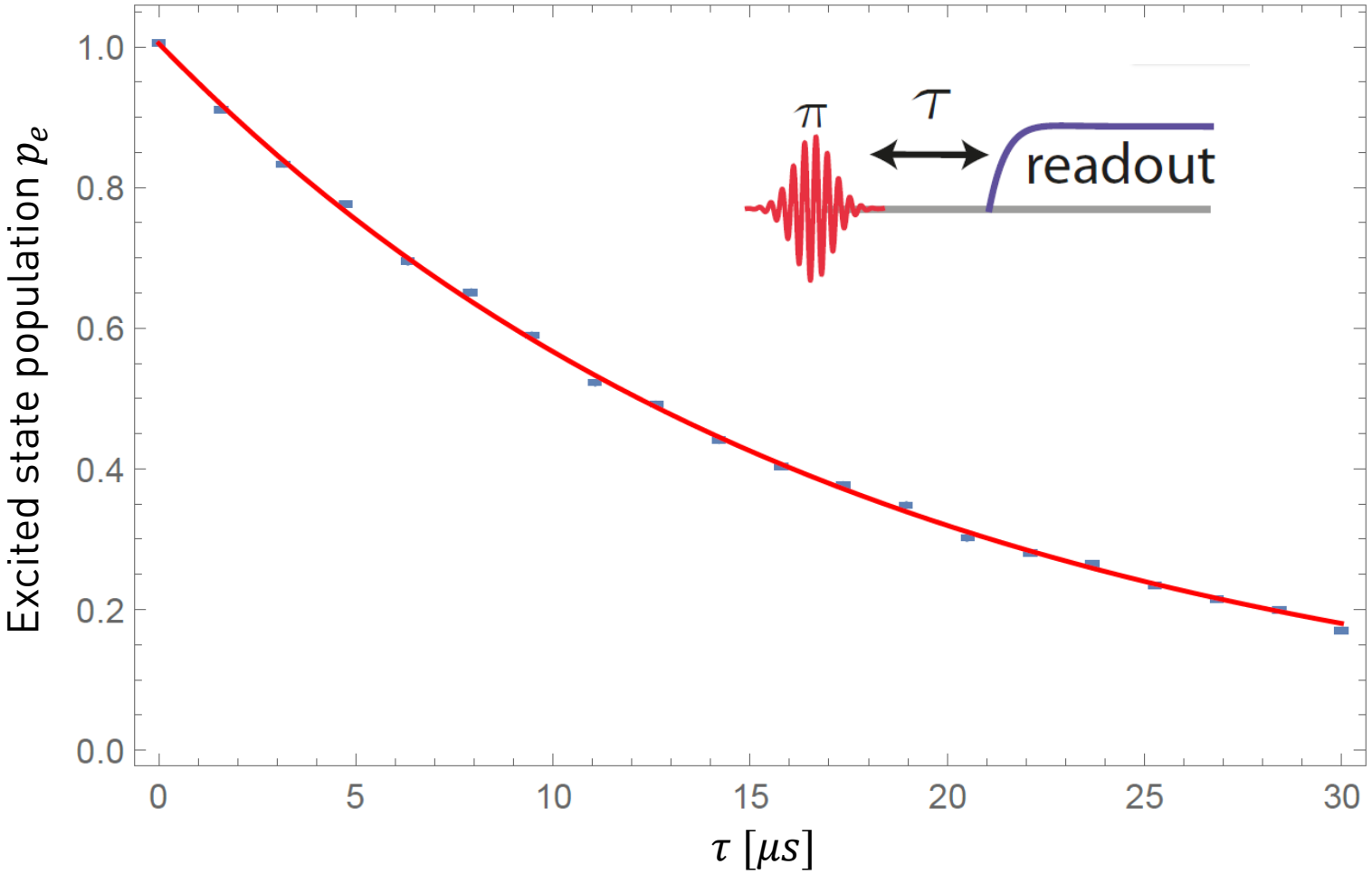

- Excite qubit with an initial π – pulse.
- Wait variable time τ before measuring the qubit population.
- Fit exponentially decaying function to extract relaxation time $T_1 \approx 18\ \mu s$.

4.10 Measurement of dephasing time

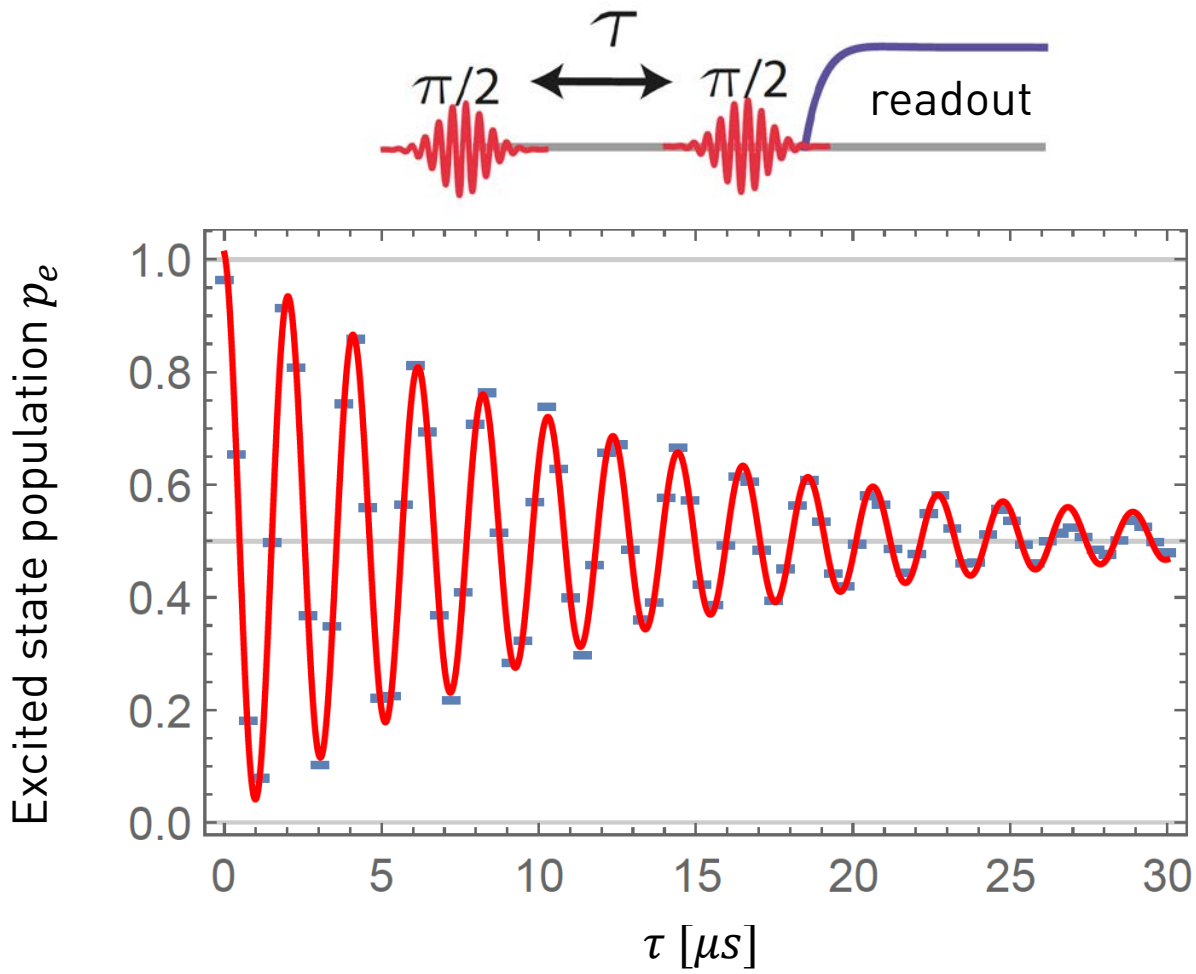

- Initial $\frac{\pi}{2}$ -pulse prepares $|g\rangle + |e\rangle$.
- Map remaining coherence after time τ to excited state using a second $\frac{\pi}{2}$- pulse, and measure.
- Detune pulse by $f_{IF} = 0.5$ MHz from qubit frequency to obtain oscillating pattern. → Higher accuracy in estimating the qubit frequency.
- Fit Characteristic decay time $T_2^* = 13\ \mu s$
- In this case, decay reasonably well described by exponential function $e^{-\tau/T_2^*}$
- Depending on spectral properties of the dominant noise source, decay better described by different functional form, e.g. Gaussian decay for 1/f – noise.
- If relaxation is only source of decoherence: $T_2 = 2\,T_1$ ("T1 limit of dephasing time").

Ithier, G. et al. PRB 72, 134519 (2005).

4.10 Measurement of dephasing time

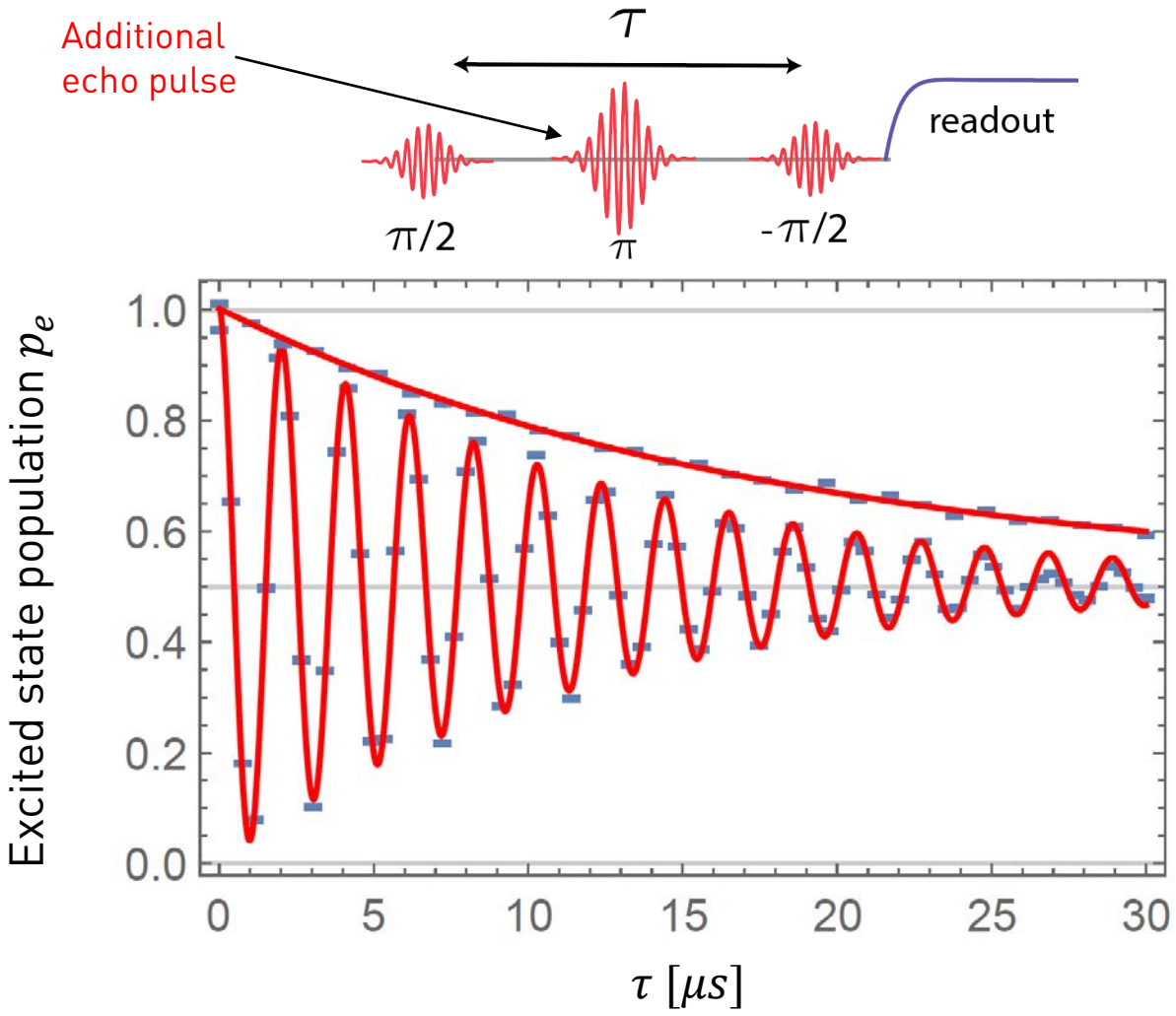

- Low frequency noise can be partly compensated for by applying an echo π-pulse after $\tau/2$ to reverse the direction of the Lamor precision.
- The resulting decay time $T_2^{echo} = 18\,\mu s$ is longer than T_2^*.
- Explanation: Low frequency noise which causes the qubit frequency to change on timescales longer than τ_{max} will cancel out.
- Variants of such dynamical decoupling sequences can be used to do noise spectroscopy → See e.g. *Bylander et al., Nat. Phys. (2011)*

Ithier, G. et al. PRB 72, 134519 (2005).

4.10 Improvements of T_1 in superconducting qubits

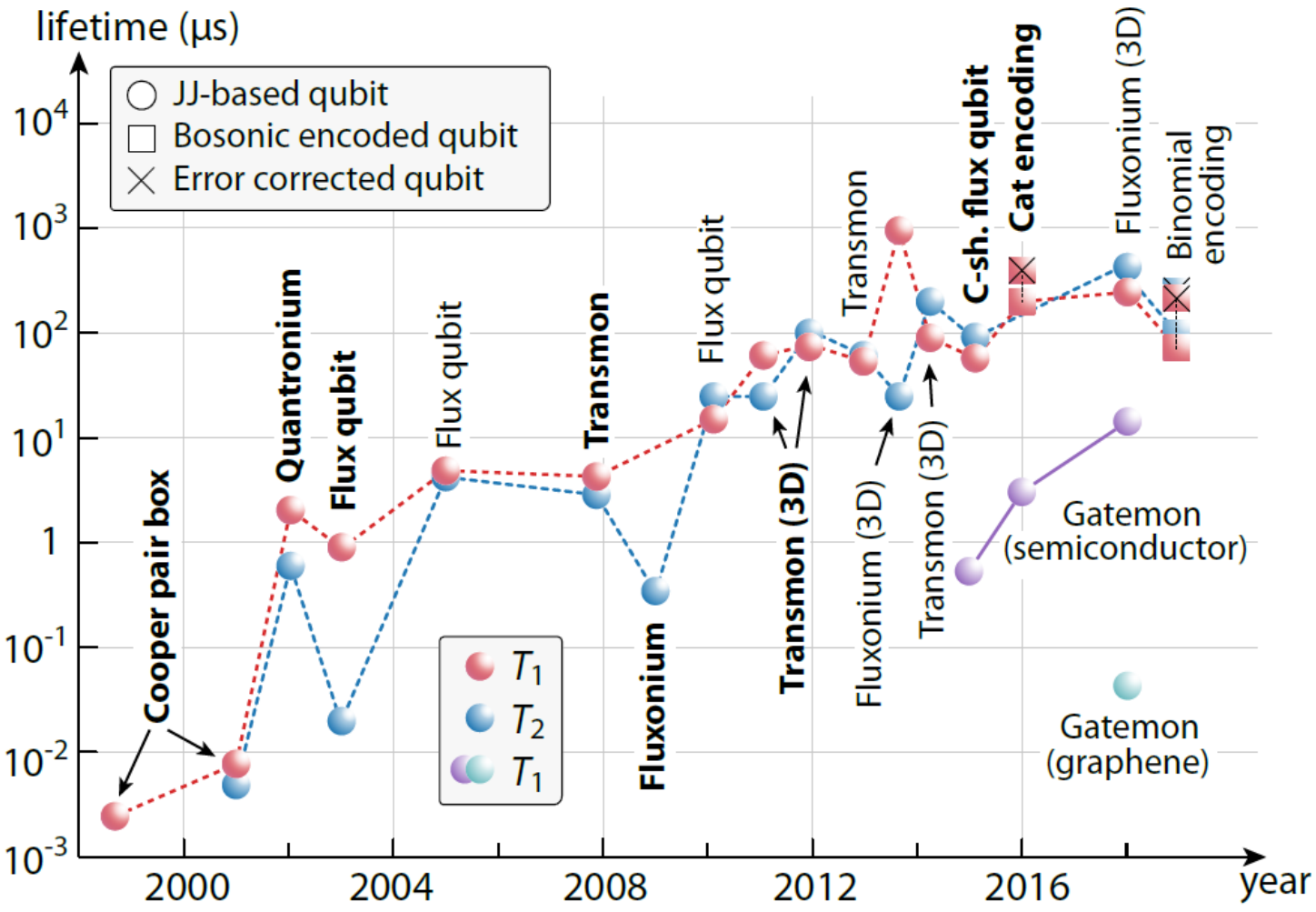

Image adopted from Kjaergaard et al., arXiv:1905.13641

4.11 Sources and mitigation of noise: A few examples

Relaxation mechanisms (T_1)

1) Radiative decay and ohmic loss due to coupling of the qubit to the electromagnetic environment.

2) Coupling to material defects described by two-level systems (TLS) mostly at the material interfaces

3) Relaxation induced by quasiparticle tunneling

4) Other sources, e.g. vortex dynamics.

Dephasing mechanisms (T_2)

1) Photon shot noise through dispersively coupled elements, e.g. residual photons in the readout circuit.

2) Magnetic flux noise in flux-tunable qubits.

3) Charge noise in combination with charge dispersion of transmon energy levels.

4.11 Relaxation due to coupling to the electromagnetic environment

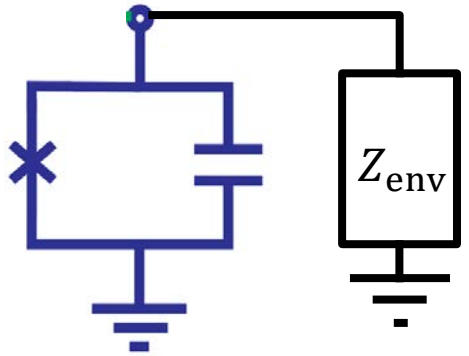

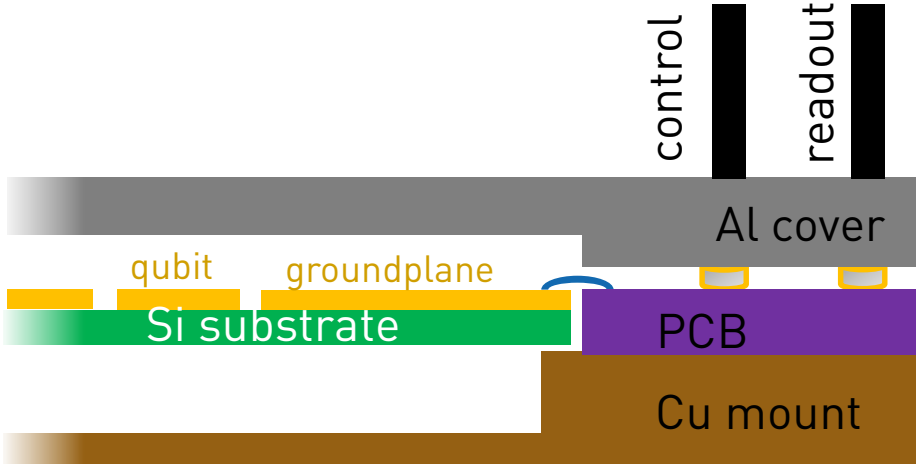

Mechanisms induced by control and readout:

- Purcell decay into readout lines. Mitigate by incorporating Purcell filters. Compare Section 4.7.
- Decay into charge control lines. Mitigate by designing coupling $\gamma \ll 1/T_1$. Compensate weaker coupling by stronger pulse.

Packaging and housing

- Resistive loss imposed by stray capacitive coupling to non-SC elements such as Cu. Avoid by designing the qubits to have well-localized mode volume; keep distance from the edge of the chip,
- Coupling to box modes of the sample enclosure, e.g. in the substrate below the qubits. Mitigate by introducing recess below chip to lift frequency of box modes. Required for larger chip size: Through Silicon Vias (TSVs) and backside metallization, and additional top chip connected via bump bonds.

4.11 Relaxation induced by two-level systems in the materials

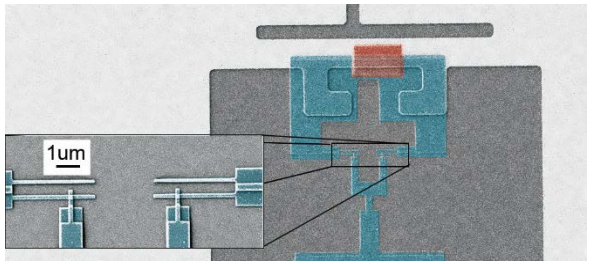

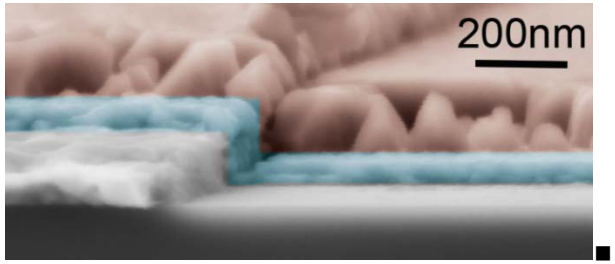

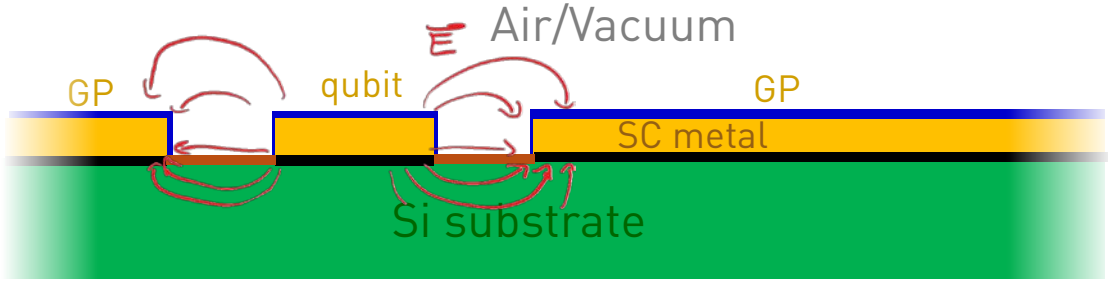

Interfaces:
Metal-Substrate (MS), Substrate-Air (SA), Metal-Air (MA)

Selected references:

Review: C. Müller et al., Rep. Prog. Phys. (2019)

Lisenfeld et al., arXiv: 1909.09749

Wang et al., PRL 107, 162601 (2015)

- Superconducting Circuits are fabricated using multiple steps of thin film deposition, lithography, etching, lift-off. Depending on the details of processing, cleaning, and choice of materials: Material defects get introduced, which mostly reside at the interfaces.
- Common model: Defects described by effective two-level systems (TLS), which couple via dipole moment to the oscillating electric field of the qubit.
- Quality factor $Q = T_1 \omega_{ge}$ of the qubit given by

$$Q^{-1} = \Sigma_i \, p_i \, \tan\delta_i$$

Sum over all materials and interfaces

- Participation ratio $p_i = \frac{\int_{V_i} \mathrm{d}V \, |E|^2}{\int_{V_{tot}} \mathrm{d}V \, |E|^2}$, can be controlled by the design of the qubit capacitors.
- Loss tangent $\tan\delta_i$ material property proportional to the density of TLS.
- Intense research efforts aim at improving the understanding of underlying physical mechanisms and to develop better fabrication processes.

4.11 Quasiparticle-induced qubit relaxation

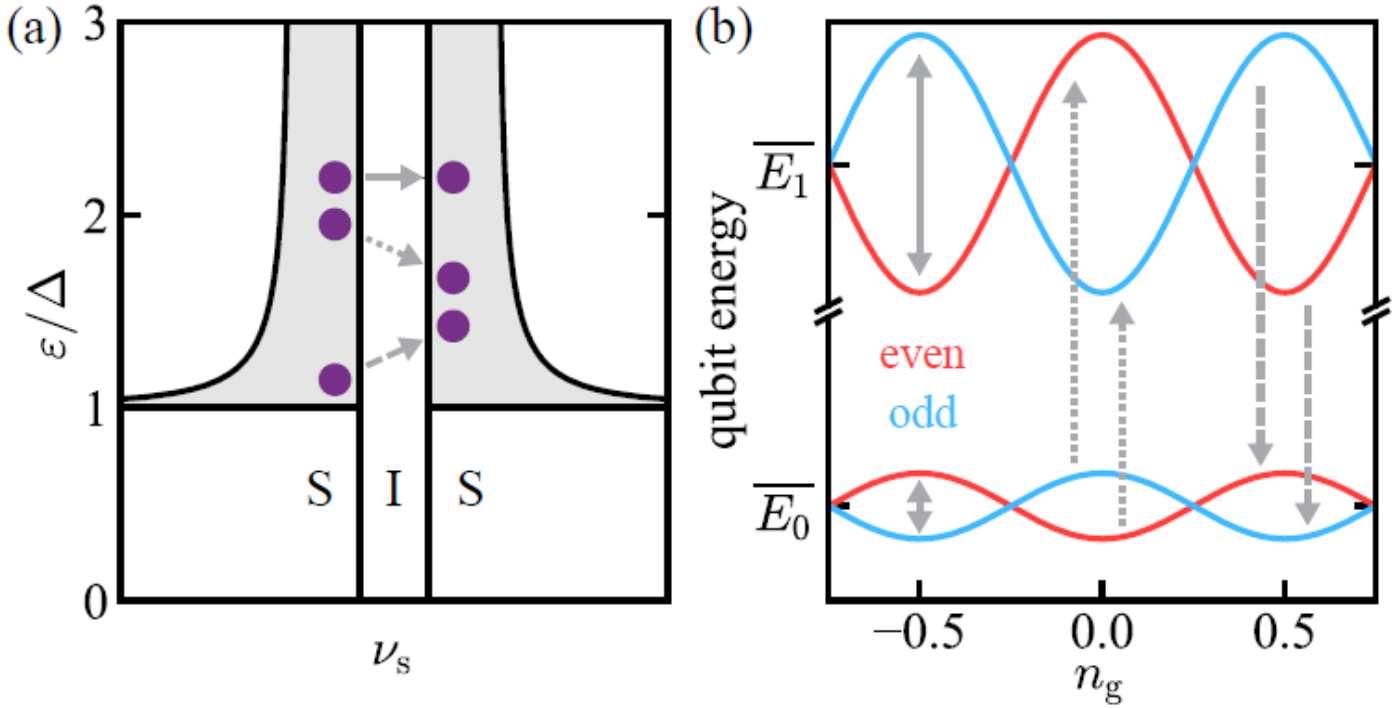

Figure from Serniak et al., PRL 121, 157701 (2018)

Further reading:

Catelani et al., PRB, (2011)

Riste et al., Nat. Comm. (2013)

Hosseinkhani et al., PRApplied (2017)

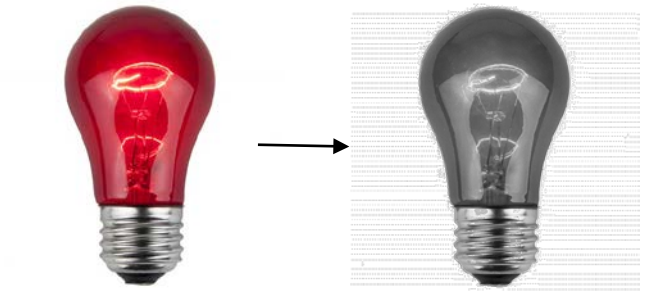

- Aluminum superconducting gap energy $2\Delta/h = 100\ \mathrm{GHz}$.
- At typical cryogenic temperature of ~20mK in thermal equilibrium quasiparticles density should be exponentially suppressed.
- Experiments find higher quasiparticle density (relative to Cooper pair density) $x_{QP} \sim 10^{-8} - 10^{-6}$.
- Tunneling of quasi particles changes parity of the offset charge and can induce qubit states transitions.
- Measured transition rates between states suggest that quasiparticles are not in thermal equilibrium.
- Mitigation: Avoid infrared (IR) radiation entering the sample box: light-tight sample enclosure, IR filter on control lines.

4.11 Sources of Dephasing: Flux noise

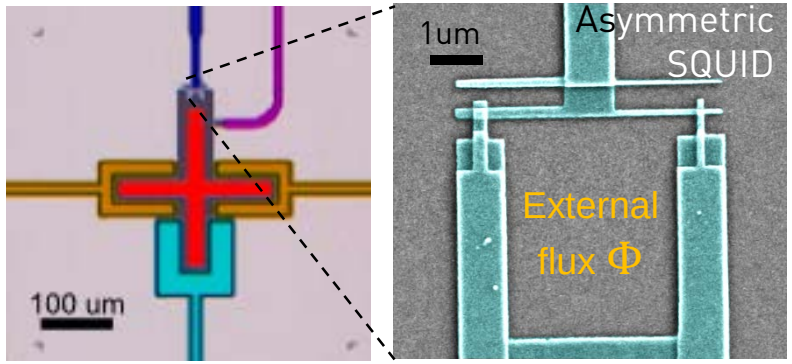

- Experiment: Measure qubit frequency ω_{ge} and T_2^* vs. external flux Φ.
- T_2^* longest at the bias points with vanishing gradient $\frac{\mathrm{d}\omega_{ge}}{\mathrm{d}\Phi} = 0$ (first order insensitive to magnetic flux noise).
- Pure dephasing rate Γ_ϕ^* is proportional to $\frac{\mathrm{d}\omega_{ge}}{\mathrm{d}\Phi}$.
- Slope proportional to flux noise density A and SQUID loop area.
- Typical values found in experiments $A \sim 10^1 - 10^3\ n\Phi_0/\mu\mathrm{m}^2$.
- Ambient magnetic noise shielded using mu-metal and superconducting cylinders around sample.
- LP and HP filters on flux control lines to suppress noise on flux control line.

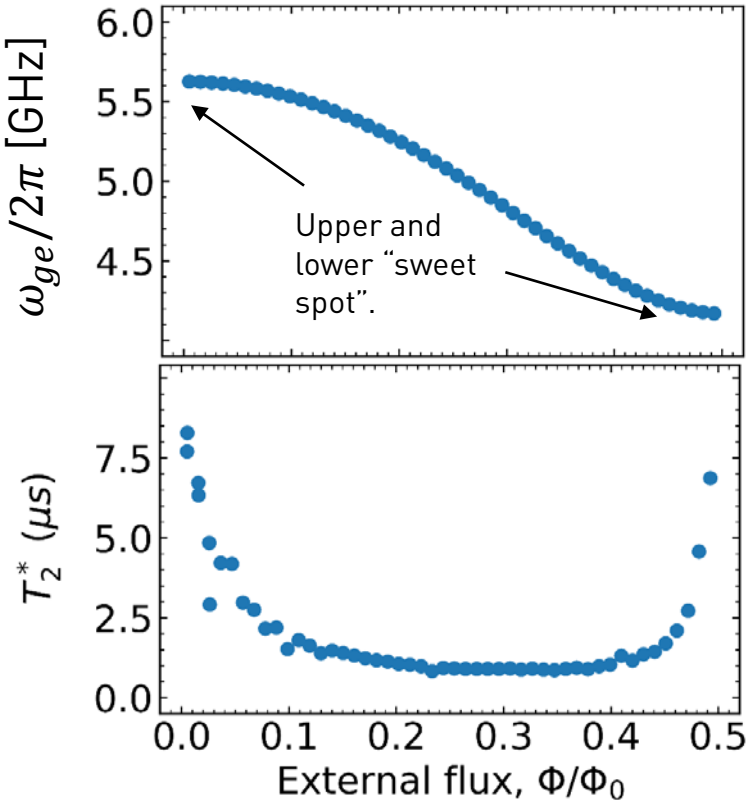

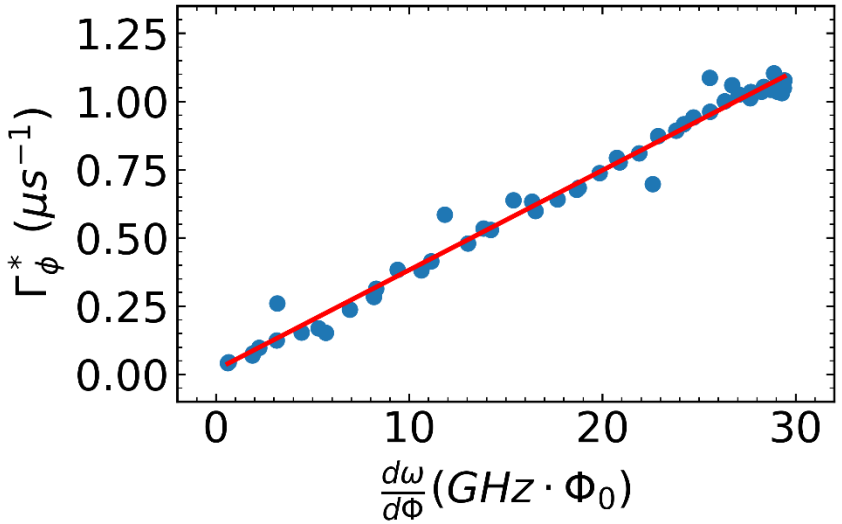

$$\frac{\Gamma_\phi^*}{2\pi} = \frac{1}{T_\phi^*} = \frac{1}{T_2^*} - \frac{1}{2T_1}$$

Compare Hutchings et al., PRApplied, 8, 044003 (2017)